IJNAOE
©SNAK, 2015

Int. J. Nav. Archit. Ocean Eng. (2015) 7:750~769
http://dx.doi.org/10.1515/ijnaoe-2015-0053
pISSN: 2092-6782, eISSN: 2092-6790

An optimal design of wind turbine and ship structure based on neuro-response surface method

Jae-Chul Lee, Sung-Chul Shin and Soo-Young Kim

Department of Naval Architecture and Ocean Engineering, Pusan National University, Busan, Korea

Received 16 December 2014; Revised 11 May 2015; Accepted 4 June 2015

ABSTRACT: *The geometry of engineering systems affects their performances. For this reason, the shape of engineering systems needs to be optimized in the initial design stage. However, engineering system design problems consist of multi-objective optimization and the performance analysis using commercial code or numerical analysis is generally time-consuming. To solve these problems, many engineers perform the optimization using the approximation model (response surface). The Response Surface Method (RSM) is generally used to predict the system performance in engineering research field, but RSM presents some prediction errors for highly nonlinear systems. The major objective of this research is to establish an optimal design method for multi-objective problems and confirm its applicability. The proposed process is composed of three parts: definition of geometry, generation of response surface, and optimization process. To reduce the time for performance analysis and minimize the prediction errors, the approximation model is generated using the Backpropagation Artificial Neural Network (BPANN) which is considered as Neuro-Response Surface Method (NRSM). The optimization is done for the generated response surface by non-dominated sorting genetic algorithm-II (NSGA-II). Through case studies of marine system and ship structure (substructure of floating offshore wind turbine considering hydrodynamics performances and bulk carrier bottom stiffened panels considering structure performance), we have confirmed the applicability of the proposed method for multi-objective side constraint optimization problems.*

KEY WORDS: Multi-objective optimization; Back-propagation artificial neural network (BPANN); Neuro-response surface method (NRSM); Non-dominated sorting genetic algorithm-II (NSGA-II); Floating offshore wind turbine; Bulk carrier bottom stiffened panels.

INTRODUCTION

The optimal engineering system design is built around the best of alternative design variables concerning system performances. Therefore, the performance evaluation is an essential process at the optimal design stage, but system performance analysis in particular is time-consuming. To solve this problem, many researchers are predicting the system performance using Response Surface Method (RSM) (Hong, 2000; Mayers and Montgomery, 1995). These RSM represent the relationship between inputs and outputs (Fig. 1). The RSM simplifies the configuration of the response surface and takes short time to generate it. In addition, it has the advantage of generating a stable response surface.

Corresponding author: *Sung-chul Shin*, e-mail: *scshin@pusan.ac.kr*

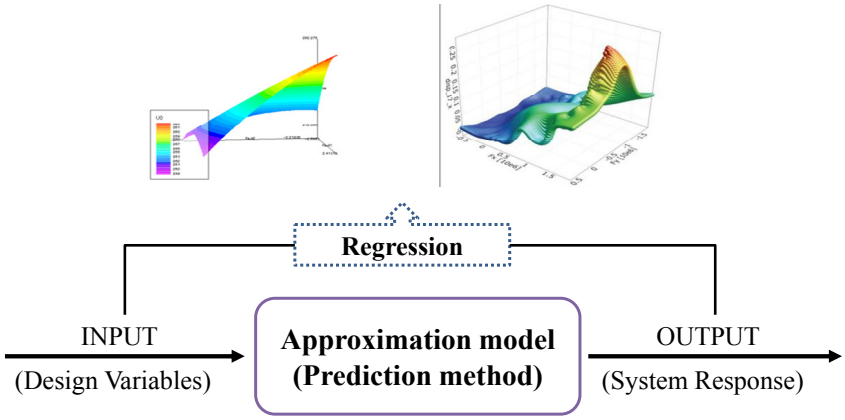

Fig. 1 Response surface method (RSM).

RSM is traditionally used to predict system performance in the engineering research field. Bucher and Bourgund employed RSM to solve structural reliability problems (Bucher and Bourgund, 1990). Kahraman developed a quadratic model for prediction and analysis of the relationship between the cutting parameters and surface roughness in the turning process of AISI 4140 steel (Kahraman, 2009), and Yu et al. (2009) studied the fatigue reliability of ship structures using RSM. However, this method produces errors in highly nonlinear problems. Marine system optimization design problems based on performance involve highly nonlinear elements, such as hydrodynamics problems (hull forms, propeller), and structural problems (superstructures, offshore structure). Therefore, many researchers have tried to increase prediction accuracy using various artificial intelligence methods. Shin employed the neuro-fuzzy algorithm to predict wake distribution (Shin, 2007), Han determined the satisfaction index of the noise using various evaluation parameters using the linear regression and back-propagation neural network algorithm (Han, 2012), and Lee et al. tried to predict the added resistance in waves using GP (Lee et al., 2014). Yang et al. (2015) studied reliability based design optimization of the tripod substructure of offshore wind turbines under dynamic constraints using the kriging method and Mandal et al. studied to predict the damage level for non-reshaped berm breakwater using ANN, SVM and ANFIS (Mandal, et al., 2012).

The application of optimization method, in NAOE optimal design problem, is time-consuming especially for performance analysis evaluation; performance prediction using approximation method can be used to reduce the evaluation time. Therefore, it is necessary to research the multi-objective optimal design framework in view of system performance in the initial design stage. In marine system optimal design problem, no research about optimization process including approximation method was found. The main objective in this study is to optimize a marine system while considering its performance, and to establish a design methodology for multi-objective optimization problems. For this purpose, we constructed a framework for optimal design based on the Neuro-Response Surface Method (NRSM) (Lee et al., 2013a). Through case study, we have confirmed the usefulness of the constructed framework in view of hydrodynamics and structural performance. The design alternatives for performance analysis are generated using an orthogonal array table (Ross, 1996), while commercial codes (AQWA, ANSYS APDL) are used for performance analysis. The framework was constructed using MATLAB code.

OPTIMAL DESIGN FRAMEWORK BASED ON NEURO-RESPONSE SURFACE METHOD (NRSM)

The proposed multi-objective optimal design framework includes two principal phases (Lee et al., 2013b):

(1st Phase)

In order to predict the system performance, the response surface is generated using the Back-Propagation Artificial Neural Network (BPANN); this process is the Neuro-Response Surface Method (NRSM).

(2nd Phase)

Optimization of system geometry using NRSM.

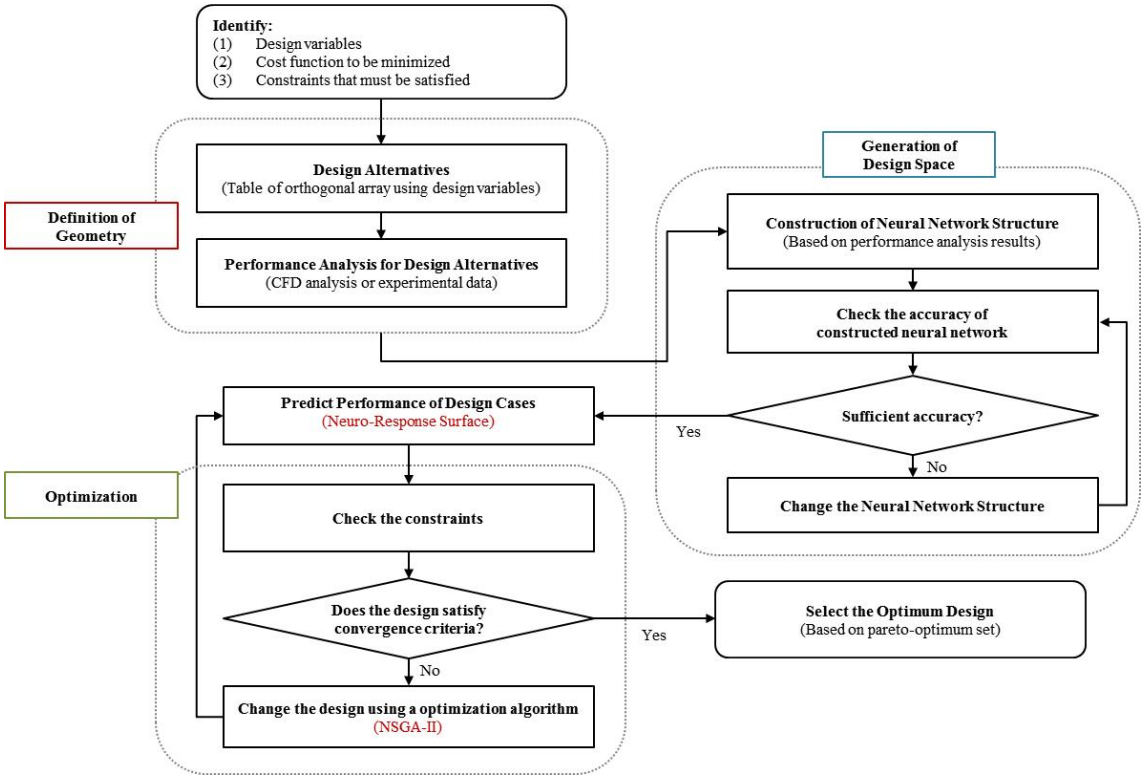

Fig. 2 Optimal design framework based on NRSM.

Fig. 2 illustrates the proposed framework which is composed of three parts:

(1st process: Definition of the geometry)

The proposed optimal design framework defines the geometry by parameterization method. An orthogonal array table is used for systematic generation of design alternatives that are divided into 2 sets:

- Training data: used to generate the response surface.
- Test data: used to check the prediction accuracy.

(2nd process: Generation of response surface using NRSM)

The response surface is generated by the Multi-Layer Perceptron (MLP). It has three layers: an input layer, hidden layer, and output layer. The back-propagation algorithm (Robert, 1989) was used to train the neural network. The optimization process is done on the generated response surface, hence the importance of its prediction accuracy. In order to construct the appropriate response surface, the best structure and the best number of learning cycles for the ANN was prepared and the prediction accuracy of the generated response surface was confirmed using 2 data sets (1st process).

(3rd process: Optimization)

The NSGA-II (Kalyanmoy, 2002) is used as a multi-objective optimization algorithm.

Finally, the optimal design can be selected using the pareto-optimum set which results from the proposed framework.

APPLICATION

The applicability of constructed optimal design framework is verified using the marine system problem considering hydrodynamics performances (5 *MW* TLP-type wind turbine substructure) and structural performance (ultimate strength of bulk carrier stiffened panel). The accuracy of the constructed framework results has been analyzed using commercial codes (AQWA and ANSYS APDL).

5 *MW* TLP-type wind turbine substructure

The objective is to decide optimal TLP-type of wind turbine substructure while considering hydrodynamics performance.

Formulation of optimization problem

The optimization problem of TLP-type wind turbine substructure while considering hydrodynamics performance (nacelle acceleration and line tension) can be formulated as: (Eqs. (1)-(2))

Find x_i
x_i = Design Variable $(i = 1, 2, 3)$
to minimize

$$F(x) = (W_1 \times f_1) + (W_2 \times f_2) \tag{1}$$

In this formula,
$f_1(x)$ = Nacelle Acceleration (g)
f_2 = Line Tension (N)
W_i = Weighting factor $(i = 1, 2)$
Subject to

$$\min x_i \le x_i \le \max x_i \tag{2}$$

where,
$i = 1, 2, 3$ (i = number of design variables)

Three design variables were considered: S (the submerged depth of a column), H (the height of the cylinder), and R_B (the cylinder radius). Fig. 3 shows the design model, including the design variables. S is set as the depth at 20% or 40% of the total area and R_C means the column radius.

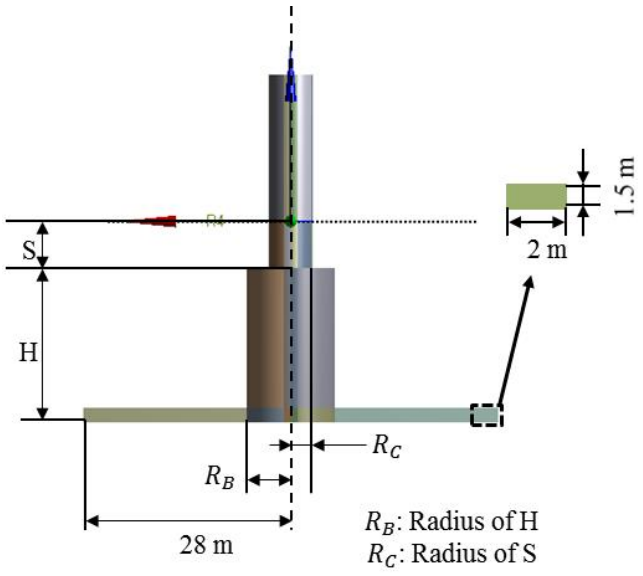

Fig. 3 Design variables.

A range of design variables S, R_B and H is presented in Table 1. In this case study, R_C is considered as fixed value.

Table 1 Range of design variables.

Design variables	Value		
R_C (m)	3 (fixed)		
R_B (m)	6	8	10
H (m)	20	25	30
S (m)	6	15	-

Environmental conditions

Table 2 shows the specifications of NREL (National Renewable Energy Laboratory) 5 *MW* wind turbine model.

Table 2 Wind turbine's specification.

Constant	Value
Wind turbine	NREL 5 *MW* Baseline Wind turbine
Wind speed	11.4 *m/s*
Turbine trust	800 *KN*
Turbine moment	72,000 *Nm*

The west coast of Korea near Chilbal-island was considered for the environmental conditions (Fig. 4). Wind speed is 11.4 (*m/s*), the significant wave height is 4.11 (*m*), the wave period is 12.49 (*sec*), and the JONSWAP spectrum is used.

Fig. 4 West coast of Korea near the island Chilbal-do.

Definition of geometry

18 set of different design alternatives were generated using an orthogonal array table ($(L_{18}(2^1 \times 3^2))$ as shown in Table 3. The case number 9 is the base design case, which is similar to the NREL 5 *MW* TLP-type wind turbine model.

Table 4 shows the results of the performance analysis for nacelle acceleration, and line tension using commercial code (AQWA).

Table 3 Design alternatives.

Case	Design variables			
	S (*m*)	R_B (*m*)	H (*m*)	Remark
1	6	6	20	-
2	15	6	20	-
3	6	6	25	-
4	15	6	25	-
5	6	6	30	-
6	15	6	30	-
7	6	8	20	-
8	15	8	20	-
9	6	8	25	Base design
10	15	8	25	-
11	6	8	30	-
12	15	8	30	-
13	6	10	20	-
14	15	10	20	-
15	6	10	25	-
16	15	10	25	-
17	6	10	30	-
18	15	10	30	-

Table 4 Results of performance analysis.

Case	S (*m*)	R_B (*m*)	H (*m*)	Nacelle acceleration (*g*)	Line tension (*N*)
1	6	6	20	0.281	1960075.875
2	15	6	20	0.243	2435565.000
3	6	6	25	0.269	2663346.250
4	15	6	25	0.235	2405806.000
5	6	6	30	0.259	2656318.000
6	15	6	30	0.225	2576460.750
7	6	8	20	0.307	3099453.750
8	15	8	20	0.258	3315056.750
9	6	8	25	0.291	3258912.250
10	15	8	25	0.246	3542092.250
11	6	8	30	0.275	3696577.000
12	15	8	30	0.236	4181562.750
13	6	10	20	0.324	4156945.750
14	15	10	20	0.268	4385337.000
15	6	10	25	0.304	3484888.000
16	15	10	25	0.255	3631862.250
17	6	10	30	0.283	6023743.000
18	15	10	30	0.243	5539120.500

After performances calculation of the generated design cases, we constructed the response surface using NRSM. Then, the performances of the various design cases can be predicted in a continuous response surface without direct computing. 15 set of data (Table 5) were used to generate the response surface. In order to check the accuracy of the constructed response surface, the results were compared using 3 set of data (Table 6). To increase the learning rate for a neural network, all data were used for a normalized value between 0.5 and 1.

Table 5 Training data.

Case	S	R_B	H	Nacelle acceleration	Line tension
1	0.500	0.500	0.500	0.780	0.500
2	1.000	0.500	0.500	0.590	0.559
4	1.000	0.500	0.750	0.551	0.555
5	0.500	0.500	1.000	0.670	0.586
6	1.000	0.500	1.000	0.500	0.576
7	0.500	0.750	0.500	0.913	0.640
9	0.500	0.750	0.750	0.832	0.660
10	1.000	0.750	0.750	0.607	0.695
11	0.500	0.750	1.000	0.754	0.714
12	1.000	0.750	1.000	0.553	0.773
14	1.000	1.000	0.500	0.714	0.798
15	0.500	1.000	0.750	0.899	0.688
16	1.000	1.000	0.750	0.649	0.706
17	0.500	1.000	1.000	0.790	1.000
18	1.000	1.000	1.000	0.589	0.940

Table 6 Test data.

Case	S	R_B	H	Nacelle acceleration	Line tension
3	0.500	0.500	0.750	0.723	0.587
8	1.000	0.750	0.500	0.665	0.667
13	0.500	1.000	0.500	1.000	0.770

Construction of approximate response surface

The number of hidden layers was changed from 1 to 10. Using six hidden layers gave a better result. Therefore, the final structure of the neural network and the number of learning cycles are 3-6-2 and 15000 respectively. The error convergence is about 0.00599 at 14000 using the constructed framework (Fig. 5).

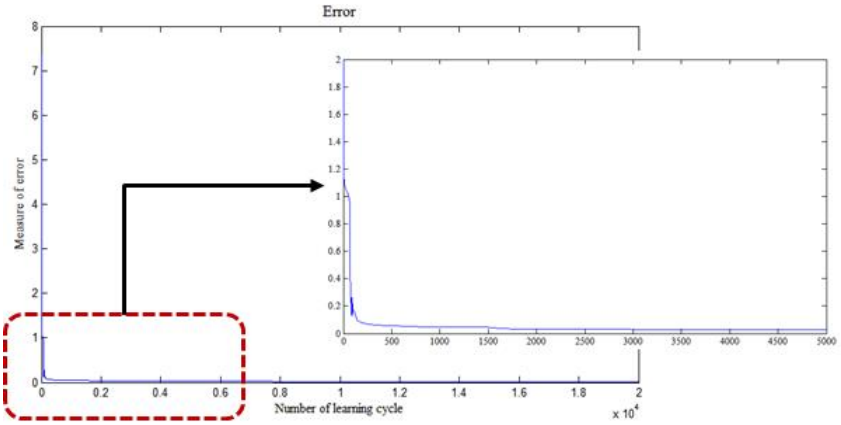

Fig. 5 Error convergence.

The error is defined in Eqs. (3) and (4). "d_j" is the output of network and "y_j" is the actual value. "L" is the number of output neurons.

$$e_j(n) = d_j(n) - y_j(n) \tag{3}$$

$$E(n) = \frac{1}{2}\sum_{j=1}^{L} e_j^{\,2}(n) \tag{4}$$

Table 7 and Fig. 6 show the learning accuracy of the trained neural network for 15 cases in the training sample. In this table, "desired values" are the AQWA analysis results, and "prediction values" are the output of the neural network. We decided that the constructed structure of the neural network is proper, because most of the error values are below 0.05 (Table 7 and Fig. 6).

Table 7 Learning accuracy of the training data set.

Case	Desired values		Prediction values	
	Nacelle acceleration	Line tension	Nacelle acceleration	Line tension
1	0.780	0.500	0.801	0.499
2	0.590	0.559	0.581	0.548
4	0.551	0.555	0.539	0.581
5	0.670	0.586	0.651	0.614
6	0.500	0.576	0.477	0.605
7	0.913	0.640	0.887	0.669
9	0.832	0.660	0.814	0.641
10	0.607	0.695	0.599	0.661
11	0.754	0.714	0.735	0.733
12	0.553	0.773	0.545	0.735
14	0.714	0.798	0.709	0.779
15	0.899	0.688	0.886	0.684
16	0.649	0.706	0.647	0.715
17	0.790	1.000	0.808	0.958
18	0.589	0.940	0.586	0.961

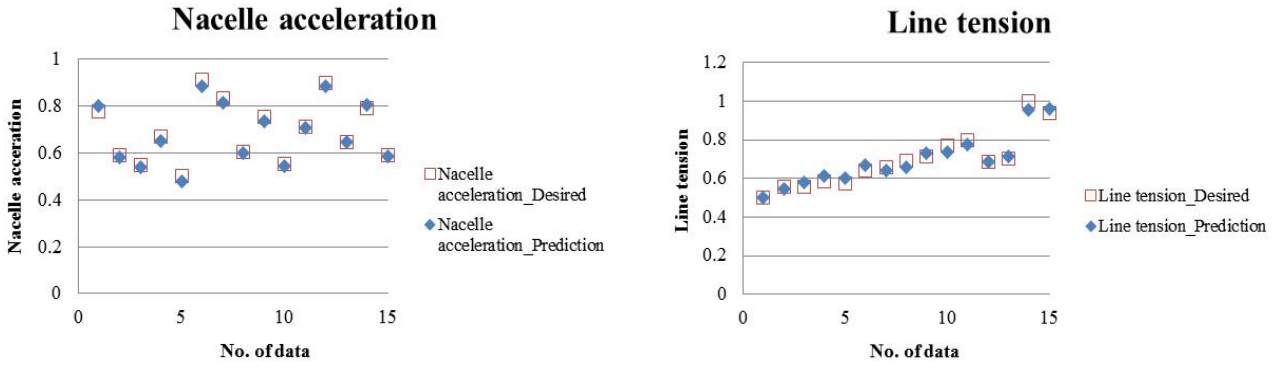

Fig. 6 Accuracy of generated response surface.

Table 8, Fig. 7 and Table 9 show the prediction accuracy and prediction error for the test data set in the generated response surface. In this process, the accuracy of the constructed response surface can be checked. Results analysis of Table 9 shows that some errors of prediction still persist. However, to deduce the performance in a limited time, the NRSM can give reasonable results. Therefore, the trained neural network was used as a performance approximation in the optimum design process.

Table 8 Prediction accuracy of the generated response surface.

Case	Desired values		Prediction values	
	Nacelle acceleration	Line tension	Nacelle acceleration	Line tension
3	0.723	0.587	0.727	0.562
8	0.665	0.667	0.649	0.695
13	1.000	0.770	0.943	0.763

Table 9 Error of test data set.

Case	Error [(Prediction value - Desired values) / Desired values]	
	Nacelle acceleration	Line tension
3	0.005	0.044
8	0.025	0.041
13	0.061	0.009

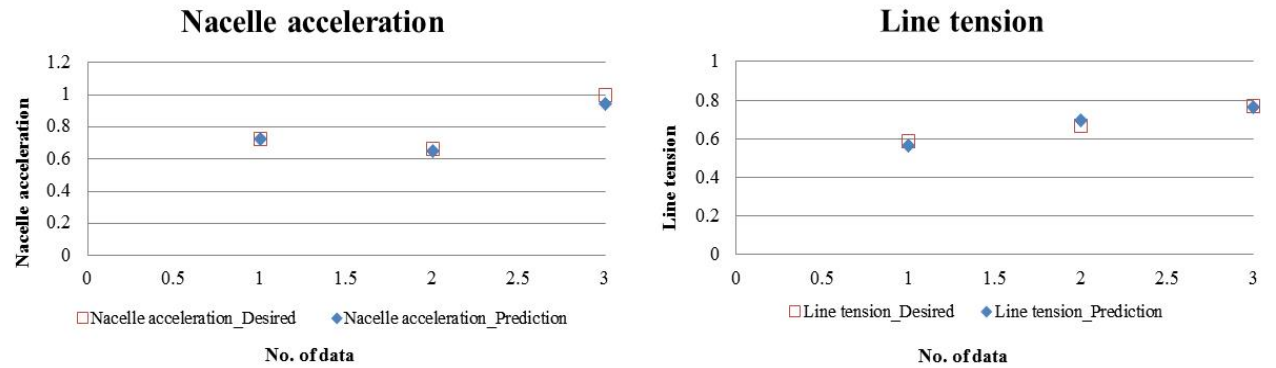

Fig. 7 Prediction accuracy results.

Optimization process based on NRSM

The optimum design can be searched using NSGA-II in the generated response surface. Table 10 shows the parameters for NSGA-II and Fig. 8 presents the pareto-optimum set as the final result of the constructed framework. In order to select the final optimum design among the pareto-optimum set, a weighting factor was used for each objective function (nacelle acceleration, and line tension). The weighting factor of the nacelle acceleration and line tension were each 0.5. In Fig. 8, the black point means the selected optimum design.

The design variables of the selected design case are S (submerged depth for a column, 14.193 *m*), H (the height of cylinder, 28.688 *m*), and R_B (Cylinder radius, 6.000 *m*).

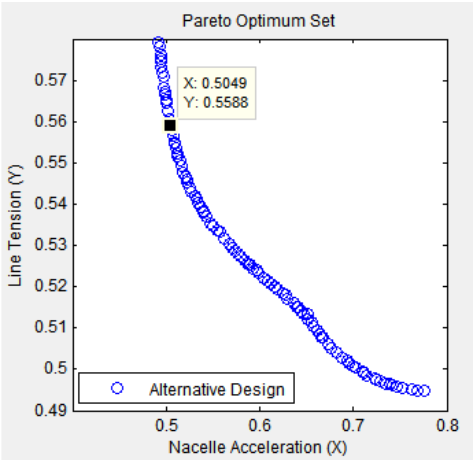

Fig. 8 Pareto-optimum set.

Table 10 Parameters.

Parameter	Value
Population size	100
Max. generation	250
Crossover	30%
Mutation	2%

Analysis of optimum design

Table 11 shows the performance analysis results between the obtained neural network and commercial code (AQWA) result. When using the constructed framework, the prediction error is up to 0.05 (line tension), as shown in Table 12. However, in order to choose the optimal design while considering its performances, the constructed framework can give reasonable results in a limited time.

Table 11 Result analysis.

Design variables for optimum design case		
S (*m*)	R_B (*m*)	H (*m*)
14.193	6.000	28.688

Results based on NRSM Framework		Results of AQWA Calculation	
Nacelle acceleration (*g*)	Line tension (*N*)	Nacelle acceleration (*g*)	Line tension (*N*)
0.226	2437987.511	0.229	2577592.750

Table 12 Prediction error.

Prediction error [(AQWA Calculation - NRSM Framework) / AQWA Calculation]	
Nacelle acceleration	Line tension
0.01	0.05

Finally, the improvement for standards of performance evaluation was analyzed as shown in Table 13, where all standards for the optimum design case decreased against the base design case.

Table 13 Improvement analysis for standards of performance evaluation.

Improvement [(Base model – Optimization model) / Base model]		
Displacement	Nacelle acceleration	Line tension
about 12% (decrease)	about 25% (decrease)	about 16% (decrease)

Fig. 9 shows the hydrodynamics performances of the optimization design case in comparison with the base design case in the frequency domain. In this graph, the red line is the base design case, and the blue line is the optimization design case. The optimized design case motions of pitch, heave, and surge are lower than in the base design case.

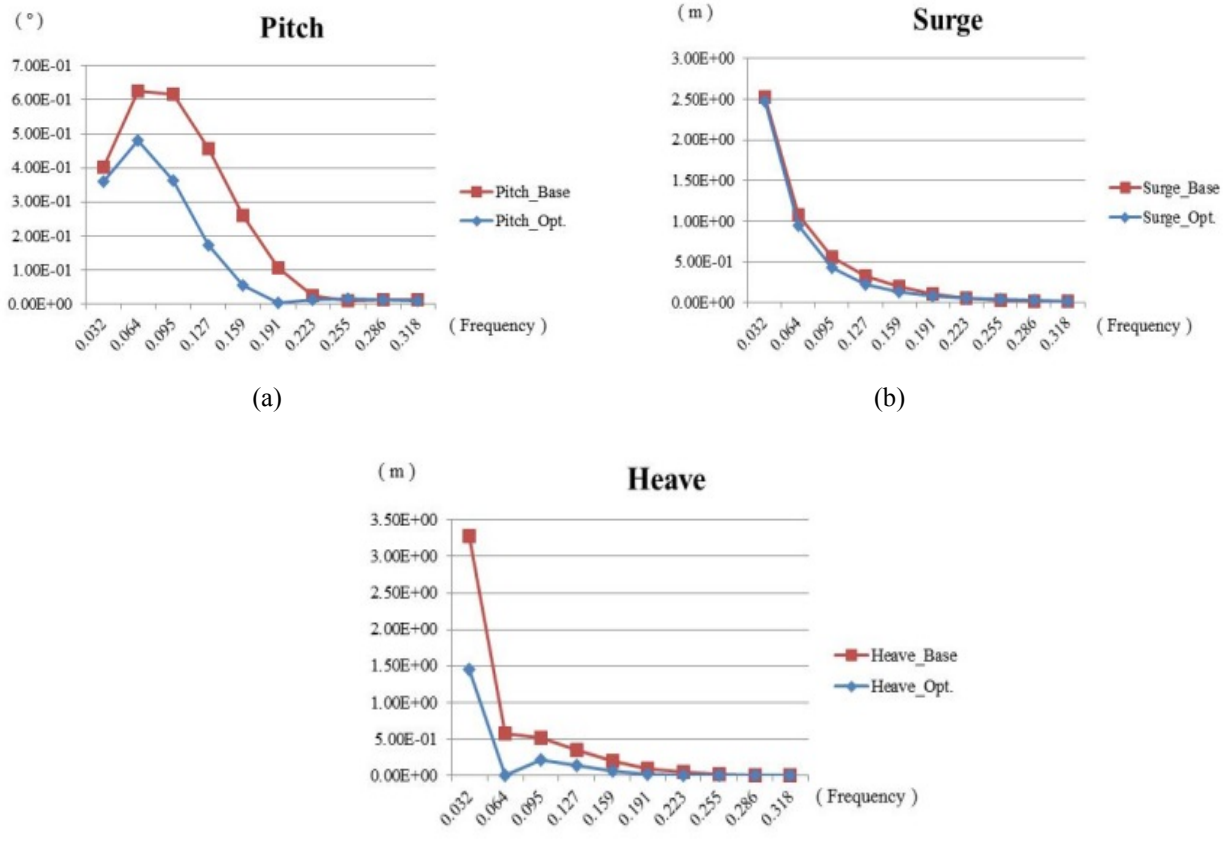

(a) (b)

(c)

Fig. 9 Performance analysis results.

Fig. 10 shows the geometry of the selected optimized model.

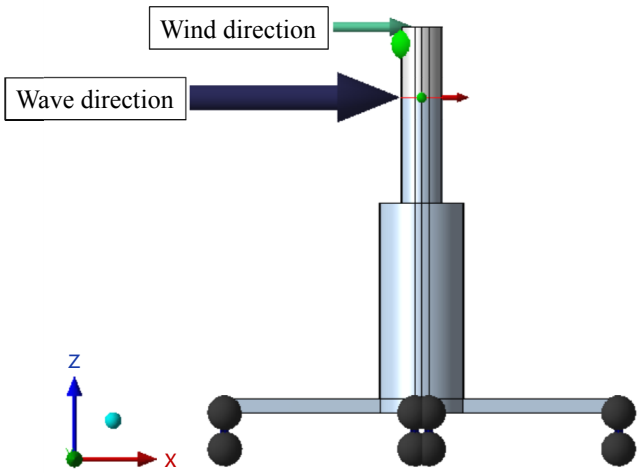

Fig. 10 Optimal sub-structure of TLP type wind-turbine.

Ultimate strength of ship stiffened panel

The objective in this case study is to decide the bulk carrier bottom stiffened panels while considering the structural performances (ultimate strength and the steel weight). Table 14 and Fig. 11 show the material and geometric properties of bulk carrier bottom stiffened panels (Kim, 2012). The Tee bar stiffener type is considered in this case study (Fig. 11).

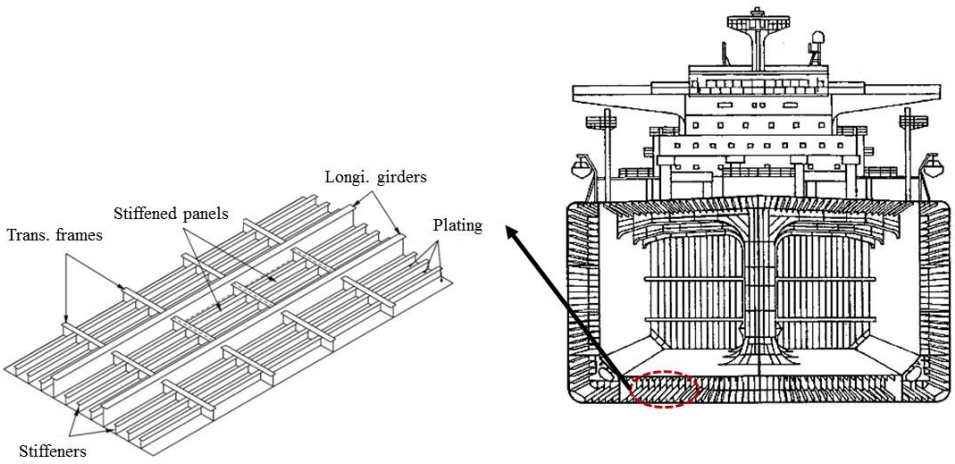

Fig. 11 Bulk carrier bottom stiffened panels.

Table 14 Material of bulk carrier bottom stiffened panels.

Yield stress of plate, σ_{YP}	313.6 N/mm^2
Yield stress of plate, σ_{YS}	313.6 N/mm^2
Elastic modulus, E	205800 N/mm^2
Poisson's ratio, ν	0.3
Plate length, a	2550 *mm*
Plate breath, b	850 *mm*
Plate thickness, t_P	9.5, 13, 16 *mm*
Number of stiffeners	2 stiffeners in a panel
No residual stress	

Formulation of optimization problem

The optimization problem of bulk carrier bottom stiffened panels while considering structural performances can be formulated as: (Eqs. (5)-(6))

Find x_i

x_i = Design Variable $(i = 1,2,3,4,5)$

to minimize

$$F(x) = (W_1 \times f_1) + (W_2 \times \frac{1}{f_2}) \tag{5}$$

In this formula,

$f_1(x)$ = Weight of steel (kg)

$f_2(x)$ = Ultimate strength (MPa)

W_i = Weighting factor $(i = 1,2)$

Subject to

$$\min x_i \le x_i \le \max x_i \tag{6}$$

where,

$i = 1,2,3,4,5$ (i = number of design variables)

Five design variables are considered: t_P (the plate thickness), t_W (the web thickness), t_f (the flange thickness), h_W (the web height) and b_f (the flange breadth). Fig. 12 shows the design model, including the design variables.

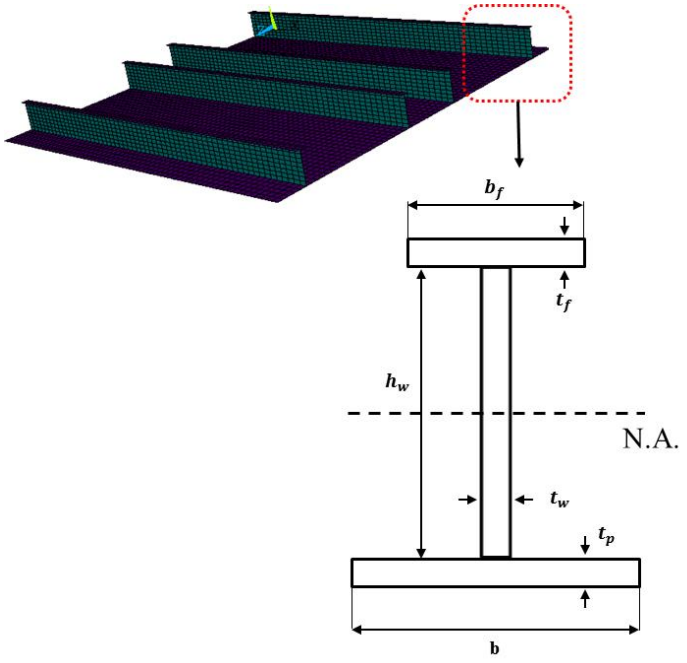

Fig. 12 Design variables.

A range of design variables $t_P, t_W, t_f, h_W, and\ b_f$ is presented in Table 15.

Table 15 Range of design variables.

Design variables	Values				
t_P (mm)	9.5	13	16	-	-
t_W (mm)	9	10	12	15	17
t_f (mm)	12	15	17	19	20
h_W (mm)	138	150	235	383	580
b_f (mm)	70	80	90	130	150

The common stiffeners of bulk carrier bottom stiffened panel are: 16 (t_P) , 383 (h_W) , 100 (b_f), 12 (t_w), and 17 (t_f). In this research, the common stiffened panel is considered as the base design case.

Analysis conditions

In this case study, the symmetric boundary condition (Table 16) (Pail and Thayamballi, 2003) was used, and two-bay model was considered as bulk carrier bottom stiffened panels (Fig. 13).

Table 16 Boundary conditions for two bay model.

Boundary	Description
A-A''' and D-D'''	Symmetric condition with $R_x = R_z = 0$ and uniform displacement in the x direction, Coupled the plate part
A-D and A'''-D'''	Symmetric condition with $R_y = R_z = 0$ and uniform displacement in the y direction, Coupled with the longitudinal stiffener
A'-D', A''-D'', B-B' and C-C'	$U_z = 0$

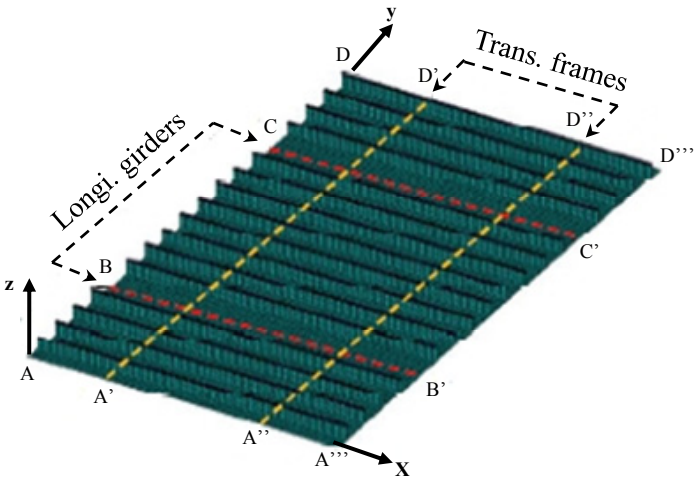

Fig. 13 Two bay model of bulk carrier bottom stiffened panels (Kim, 2012).

In case of structural analysis using non-linear analysis method, the pressure which depends on the direction of the lateral pressure can be divided into plate-side pressure and stiffened-side pressure (Kim, 2012). The stiffened-side pressure was considered in this research (Fig. 14).

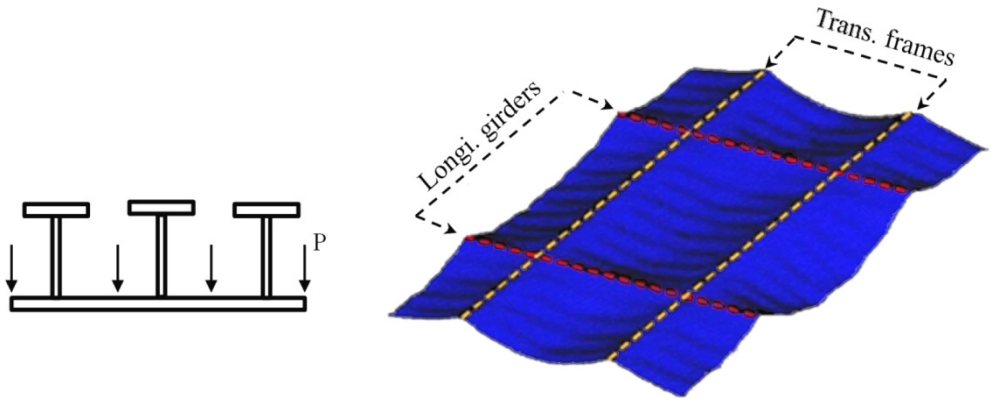

Fig. 14 Stiffened-side pressure (Kim, 2012).

Definition of geometry

15 set of different design alternatives were generated using an orthogonal array table. A modified 3-level L 15 array was used to generate the alternative designs. Table 17 shows the design alternatives and the results of the performance analysis for a steel weight and ultimate strength of bottom stiffened panels using commercial code (ANSYS APDL).

Table 17 Design alternatives & Results of performance analysis.

Case	t_P (mm)	t_W (mm)	t_f (mm)	h_W (mm)	b_f (mm)	Steel weight (kg)	Ultimate strength (MPa)
1	9.5	9.0	12.0	138.0	70.0	1797.295	0.531
2	9.5	10.0	15.0	150.0	80.0	1896.766	0.520
3	9.5	12.0	17.0	235.0	90.0	2162.343	0.575
4	9.5	15.0	19.0	383.0	130.0	2784.438	0.714
5	9.5	17.0	20.0	580.0	150.0	3532.079	0.906
6	13.0	9.0	15.0	235.0	130.0	2655.170	0.428
7	13.0	10.0	17.0	383.0	150.0	3027.784	0.499
8	13.0	12.0	19.0	580.0	70.0	3335.210	0.651
9	13.0	15.0	20.0	138.0	80.0	2591.593	0.739
10	13.0	17.0	12.0	150.0	90.0	2585.155	0.719
11	16.0	9.0	17.0	580.0	80.0	3521.717	0.497
12	16.0	10.0	19.0	138.0	90.0	2959.981	0.969
13	16.0	12.0	20.0	150.0	130.0	3170.833	1.122
14	16.0	15.0	12.0	235.0	150.0	3319.718	1.229
15	16.0	17.0	15.0	383.0	70.0	3679.615	1.296

15 set of data (Table 18) were used to generate the response surface and 3 set of data (Table 19) were used to check the accuracy of the constructed response surface. In order to increase the learning rate for a neural network, all data were used for a normalized value between 0.5 and 1.

Table 18 Training data.

Case	t_P	t_W	t_f	h_W	b_f	Steel weight	Ultimate strength
1	0.500	0.500	0.500	0.500	0.500	0.500	0.856
2	0.500	0.563	0.688	0.514	0.563	0.526	0.868
3	0.500	0.688	0.813	0.610	0.625	0.597	0.809
4	0.500	0.875	0.938	0.777	0.875	0.762	0.701
5	0.500	1.000	1.000	1.000	1.000	0.961	0.606
6	0.769	0.500	0.688	0.610	0.875	0.728	1.000
7	0.769	0.563	0.813	0.777	1.000	0.827	0.894
8	0.769	0.688	0.938	1.000	0.500	0.909	0.744
9	0.769	0.875	1.000	0.500	0.563	0.711	0.686
10	0.769	1.000	0.500	0.514	0.625	0.709	0.698
11	1.000	0.500	0.813	1.000	0.563	0.958	0.896
12	1.000	0.563	0.938	0.500	0.625	0.809	0.583
13	1.000	0.688	1.000	0.514	0.875	0.865	0.538
14	1.000	0.875	0.500	0.610	1.000	0.904	0.513
15	1.000	1.000	0.688	0.777	0.500	1.000	0.500

Table 19 Test data.

Case	t_P	t_W	t_f	h_W	b_f	Steel weight	Ultimate strength
1’	0.538	0.625	0.563	0.502	0.531	0.539	0.937
2’	0.692	0.750	0.750	0.570	0.656	0.689	0.660
3’	0.923	0.938	0.875	0.740	0.813	0.968	0.565

Construction of approximate response surface

In this case study, the optimal structure of the neural network and the number of learning cycles are 5-8-2 and 2200 respectively. The error convergence is about 0.006 at 1943 using the constructed framework (Fig. 15).

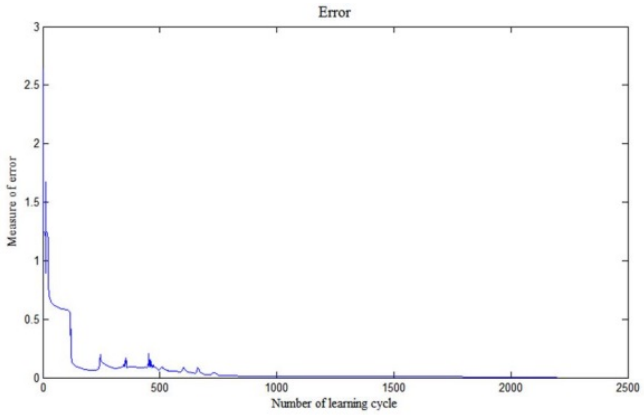

Fig. 15 Error convergence.

Table 20 shows the learning accuracy of the trained neural network for 15 cases in the training sample. We decided that the structure of the neural network is proper, because most of the error values are below 0.08, and the results for the neural network learning were appropriate (Table 20). In this table, "desired values" are the ANSYS APDL analysis results, and "prediction values" are the output of the neural network.

Table 21 shows the prediction accuracy of the trained neural network and Table 22 shows the prediction error of test data. In this table, the error is below 0.15. Therefore, prediction accuracy of the performance can give reasonable values.

Table 20 Learning accuracy of the training data set.

Case	Desired values		Prediction values	
	Steel weight	Ultimate strength	Steel weight	Ultimate strength
1	0.500	0.856	0.486	0.897
2	0.526	0.868	0.519	0.862
3	0.597	0.809	0.585	0.838
4	0.762	0.701	0.745	0.802
5	0.961	0.606	0.928	0.702
6	0.728	1.000	0.694	0.955
7	0.827	0.894	0.825	0.932
8	0.909	0.744	0.902	0.785
9	0.711	0.686	0.690	0.711
10	0.709	0.698	0.715	0.698
11	0.958	0.896	0.962	0.894
12	0.809	0.583	0.841	0.547
13	0.865	0.538	0.861	0.498
14	0.904	0.513	0.905	0.512
15	1.000	0.500	0.965	0.505

Table 21 Prediction accuracy of the generated response surface.

Case	Desired values		Prediction values	
	Steel weight	Ultimate strength	Steel weight	Ultimate strength
1'	0.500	0.856	0.486	0.897
2'	0.526	0.868	0.519	0.862
3'	0.597	0.809	0.585	0.838

Table 22 Error of test data set.

Error [(desired value-prediction value) / desired value]	
Steel weight	Ultimate strength
0.008	0.154
0.007	0.055
0.029	0.145

Optimization process based on NRSM

Table 23 and Fig. 16 show the parameters for NSGA-II and the pareto-optimum set as the final result of the constructed framework. In order to select the final optimum design among the pareto-optimum set, the weighting factor of the ultimate strength and steel weight were each 0.5. In Fig. 16, the black point means the selected optimum design.

The design variables of the selected design case are t_P (the plate thickness, 9.5 *mm*), t_W (the web thickness, 15.7 *mm*), t_f (the flange thickness, 13.5 *mm*), h_W (the web height, 138 mm) and b_f (the flange breadth, 148.9 *mm*).

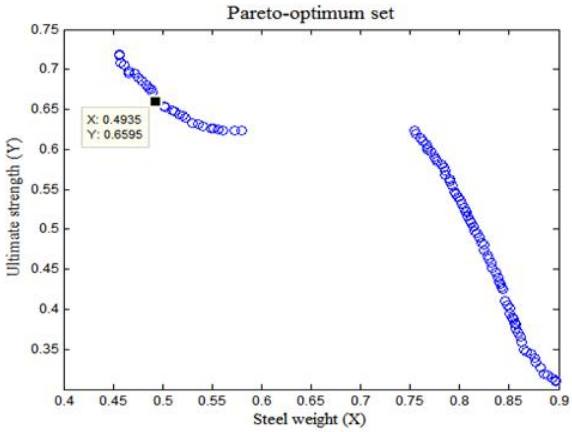

Fig. 16 Pareto-optimum set.

Table 23 Parameters.

Population	100
Crossover	20%
Mutation	1%
Max. Generation	250

Analysis of optimum design

Table 24 shows the structural analysis results between the obtained neural network and commercial code (ANSYS APDL) result. When using the constructed framework, the prediction error is up to 0.17 (steel weight), as shown in Table 25. But, in order to choose the optimal design while considering performances, the constructed framework can give reasonable results in an initial design process.

Table 24 Result analysis.

(a) Design variables.

Design variables for optimum design case				
t_P (mm)	t_W (mm)	t_f (mm)	h_W (mm)	b_f (mm)
9.5	15.7	13.5	138.0	148.9

(b) Performance results.

Results based on NRSM Framework		Results for APDL Calculation	
Steel weight (*Kg*)	Ultimate strength (*MPa*)	Steel weight (*kg*)	Ultimate strength (*MPa*)
1772.783	0.787	2136.553	0.728

Table 25 Prediction error.

Prediction error [(APDL Calculation - NRSM Framework) / APDL Calculation]	
Steel weight	Ultimate strength
0.17	0.08

Finally, the improvement of performance evaluation standards was analyzed as shown in Table 26, where all standards for the optimum design case are better than the base design case.

Table 26 Improvement analysis for standards of performance evaluation.

Improvement [(Base model – Optimization model) / Base model]	
Steel weight (*kg*)	Ultimate strength (*Mpa*)
0.385 (Decrease)	0.121 (Increase)

CONCLUSION

The following conclusions were obtained in this study:

1) We proposed an optimal design framework based on the neuro-response surface method (NRSM):
   - To generate the response surface, this method uses the backpropagation artificial neural network (BPANN) that is considered as NRSM in the proposed framework.
   - The system is optimized using the non-dominated sorting genetic algorithm (NSGA-II).
   - The final optimum design case is chosen using the weighting factor for each objective function;

2) The proposed framework is considered as the useful marine system optimization design tool, in the initial design stage:
   - Save the performance analysis time in the optimization process;
   - Widely check the alternative design case.

In future research, we will evaluate the effectiveness and usefulness for proposed design framework through application of various geometry optimization problems for naval architecture and ocean engineering.

ACKNOWLEDGEMENTS

This work was supported by the National Research Foundation of Korea (NRF) grant funded by the Korea government (MEST) through GCRC-SOP (No. 2011-0030671).

REFERENCES

Bucher, C.G. and Bourgund, U., 1990. A fast and efficient response surface approach for structural reliability problem. *Structural Safety*, 7(1), pp.57-66.

Han, H.S., 2012. Psycho-acoustic evaluation of the indoor noise in cabins of a navalvessel using a back-propagation neural network algorithm. *International Journal of Naval Architecture and Ocean Engineering*, 4(4), pp.374-385.

Hong, K.J., Jeon, K.K., Sho, Y.S., Choi, D.H., Lee, S.J., 2000. A study on the construction of response surfaces for design optimization. *Trans. Korea Soc. Mech. Eng, A*, 24(6), pp.1408-1418.

Kahraman, F., 2009. The use of response surface methodology for prediction and analysis of surface roughness of aisi 400 steel. *Materials and technology*, 43(5), pp.267-270.

Kalyanmoy, D., 2002. A fast and elitist multiobjective genetic algorithm: NSGA-II. *IEEE Transaction on evolutionary computation*, 6(2), pp.182-197.

Kim, S.J., 2012. *A benchmark study on ultimate strength analysis methods of ship stiffened panel.* Thesis for the degree of Master of Science, Pusan National University (in Korean).

Lee, J.C., Shin, S.C. and Kim, S.Y., 2013a. Development of framework for NRSM based optimal shape design. *Proceedings of KIIS Spring Conference 2013*, 23(1), pp.3-4 (in Korean).

Lee, J.C., Shin, S.C. and Kim, S.Y., 2013b. A study on the development and the verification of engineering structural design framework based on Neuro-Response Surface Method (NRSM). *Journal of Korean Institute of Intelligent Systems*, 24(1), pp.46-51 (in Korean).

Lee, J.C., Jeong, J.H., and Shin, S.C., 2014. A study on prediction method for added resistance in waves using the Genetic Programming. *Proceedings of the Annual Autumn Conference*, Changwon, 06-07 November 2014, pp.482-490.

Mandal, S., Rao, S., Harish, N. and Lokesha, 2012. Damage level prediction of non-reshaped berm breakwater using ANN, SVM and ANFIS models. *International Journal of Naval Architecture and Ocean Engineering*, 4, pp.112-122.

Mayers, R.H. and Montgomery, D.C., 1995. *Response surface methodology – process and product optimization using Designed experiments.* New York: John Wiley & Sons.

Pail, J.K. and Thayamballi, A.K., 2003. *Ultimate limit state design of steel-plated structures.* Chichester: John Wiley&Sons.

Robert, H.N., 1989. Theory of the back-propagation neural network. *International Joint Conference*, 1, pp.593-605.

Ross, P.J., 1996. *Taguchi techniques for quality engineering.* 2nd. CA: McGraw-Hill Professional Publishing.

Shin, S.C., 2007. A study on prediction of wake distribution by Neuro-Fuzzy system. *International Journal of Fuzzy Logic and Intelligent systems*, 17(2), pp.154-159 (in Korean).

Yang, H., Zhu, Y., Lu, Q. and Zhang, J., 2015. Dynamic reliability based design optimisation of the tripod sub-structure of offshore wind turbines. *Renewable Energy*, 78, pp.16-25.

Yu, L., Das, P.K. and Zheng, Y., 2009. A response surface approach to fatigue reliability of ship structures. *Ships and Offshore Structures*, 4(3), pp.253-259.